Biochemistry and Biophysics Reports 23 (2020) 100776

Contents lists available at ScienceDirect

Biochemistry and Biophysics Reports

journal homepage: www.elsevier.com/locate/bbrep

The dynamic structure of Rab35 is stabilized in the presence of GTP under physiological conditions

Takuya Murata [a], Yuka Unno [a], Mitsunori Fukuda [b], Naoko Utsunomiya-Tate [a,*]

[a] Faculty of Pharma-Science, Teikyo University, 2-11-1, Kaga, Itabashi-ku, Tokyo, 173-8605, Japan
[b] Laboratory of Membrane Trafficking Mechanisms, Department of Integrative Life Sciences, Graduate School of Life Sciences, Tohoku University, Aobayama, Aoba-ku, Sendai, Miyagi, 980-8578, Japan

ARTICLE INFO

Keywords:
Rab35
Circular dichroism spectroscopy
Secondary structure
α-Helix
Guanosine triphosphate

ABSTRACT

Rab proteins, a family of small guanosine triphosphatases, play key roles in intracellular membrane trafficking and the regulation of various cellular processes. As a Rab isoform, Rab35 is crucial for recycling endosome trafficking, cytokinesis and neurite outgrowth. In this report, we analyzed dynamic structural changes and physicochemical features of Rab35 in response to different external conditions, including temperature, pH, salt concentration and guanosine triphosphate (GTP), by circular dichroism (CD) spectroscopy. CD spectra revealed that the α-helix content of Rab35 varies under different conditions considerably. The addition of GTP increases the α-helix content of Rab35 when the temperature, pH and salt concentration match physiological conditions. The results suggest that the external environment affects the secondary structure of Rab35. In particular, the presence of GTP stabilized the α-helices of Rab35 under physiological conditions. These structural changes may translate to changes in Rab35 function and relate to its role in membrane trafficking.

1. Introduction

Rab guanosine-5′-triphosphotases (GTPases) play important roles in intracellular membrane trafficking, and are thus involved in the regulation of various cellular processes [1–5]. These proteins function as switch molecules, cycling between the guanosine triphosphate (GTP)-bound active form and the guanosine diphosphate (GDP)-bound inactive form. The switch from the inactive to active state is mediated by the guanine-nucleotide exchange factor (GEF), whereas the GTPase-activating protein (GAP) mediates the reverse process of switching from the active to inactive state [6–8]. In the active form, Rab GTPases are localized at the intracellular membrane where they interact with effector proteins involved in membrane trafficking functions [9,10]. The interaction between Rab GTPases and effector proteins is highly specific, facilitating each trafficking event and cellular process. Therefore, mutation or dysfunction of Rab GTPases is associated with various human diseases, such as neurological diseases and cancer [11,12].

About 60 Rab GTPase isoforms have been identified in mammals. Rab35 is a key regulator of endocytic recycling toward the plasma membrane [13] and is therefore involved in various cellular processes, such as the maintenance of cell polarity, cytokinesis, cell adhesion and neurite outgrowth [13–17]. In the active state, Rab35 interacts with various effector proteins [6], such as centaurin-β2 (also known as ACAP2) [16,17]; RUSC2, RUN and SH3 domain containing 2 [18]; and OCRL, oculocerebrorenal syndrome of Lowe [19]. Centaurin-β2 interacts with Rab35 predominantly in the active form. Recognition of Rab35 by centaurin-β2 is necessary for nerve growth factor (NGF)-induced neurite outgrowth of neuronal cells. Alternatively, the interaction between RUSC2 and Rab GTPases is also significant for NGF-induced neurite outgrowth. The crystal structures of Rab35 in complex with the effector proteins centaurin-β2 and RUSC2 were recently reported [20]. The effector protein, OCRL, is a phosphatidylinositol-4, 5-bisphosphate (PtdIns(4,5)P_2) 5-phosphatase that interacts with Rab35 to regulate cytokinesis abscission.

The amino acid sequence of the Rab GTPase family is highly conserved. The crystal structures of Rab1a (PDB ID: 2FOL) and Rab3a (PDB ID: 3RAB) from the Rab GTPase family have been solved, and other Rab GTPase isoforms are considered to have the same structures [8,21]. The structure of all Rab GTPase isoforms includes a conserved globular G-domain, as found in Ras GTPase, and adopts a α/β-fold consisting of five α-helices and six β-sheets (Fig. 1) [8,21]. Furthermore, two GTP-sensitive domains, the switch-I and switch-II regions, exist in the G-domain (Fig. 1). Although GTP binding stabilizes the switch-I and

* Corresponding author. Faculty of Pharma-Science, Teikyo University, 2-11-1, Kaga, Itabashi-ku, Tokyo, 173-8605, Japan.
E-mail address: tate@pharm.teikyo-u.ac.jp (N. Utsunomiya-Tate).

https://doi.org/10.1016/j.bbrep.2020.100776
Received 5 March 2020; Received in revised form 18 May 2020; Accepted 20 May 2020

switch-II regions, the two regions are destabilized and relaxed by nucleotide hydrolysis and Pi release, resulting in the GDP-bound state [8]. Despite the structural similarity, local structural differences among Rab GTPase isoforms arise from differences among the amino acid sequences, and these subtle structural characteristics modulate their functions. Conformational changes that occur during the transition from the GTP-bound form to the GDP-bound form promote specific interactions of Rab GTPases with effector proteins in the GTP-bound active form. However, dynamic structural changes to Rab GTPases caused by the surrounding conditions remain unclear.

In this study, we examined dynamic structural changes to Rab35 under various environmental conditions, including temperature, pH and salt concentration, using circular dichroism (CD) spectroscopy. Furthermore, we investigated the effect of GTP on the structure of Rab35. Our results demonstrated that the proportion of α-helix and β-sheet content in Rab35 changed in an environment-dependent manner. In particular, the α-helix content was affected by the environmental conditions. Furthermore, we show that the α-helix structure was stabilized by the addition of GTP.

2. Materials and methods

2.1. Reagents

GTP was purchased from Wako Pure Chemical Industries (Osaka, Japan). GTPγS was purchased from Sigma-Aldrich (St. Louis, MO, USA).

2.2. Protein expression and purification

The full-length mouse Rab35 cDNA was prepared using *Bam*HI and *Not*I from pGEX-4T-3-Rab35, as described previously [18]. For bacterial expression of the protein, full-length mouse Rab35 cDNA was inserted into the pET28a(+) plasmid vector (Novagen, Darmstadt, Germany).

Recombinant Rab35 was expressed as an N-terminal His_6-tagged protein in an *Escherichia coli* BL21 (DE3) strain (Wako Pure Chemical Industries) via 1 mM isopropyl-β-D-thiogalactoside (IPTG) induction at 15 °C overnight. Harvested cells were resuspended in sonic buffer (20 mM Tris-HCl (pH 8.0), 500 mM NaCl and 1 mM phenylmethylsulfonyl fluoride (PMSF)) and disrupted by sonication. The lysate was centrifuged at 15,000 *g* and 4 °C for 20 min. The supernatant was loaded onto Ni^{2+}–NTA agarose resin (Roche) and incubated for 2 h at 4 °C. After washing with the wash buffer (20 mM Tris-HCl (pH 8.0), 100 mM NaCl and 1 mM PMSF), the N-terminal His_6-tagged Rab35 protein was eluted with the elution buffer (20 mM Tris-HCl (pH 8.0), 100 mM NaCl, 300 mM imidazole and 1 mM PMSF). The protein sample was dialyzed against buffer (20 mM Tris-HCl (pH 8.0) and 100 mM NaCl) and loaded onto an anion-exchange column (Mono Q 10/100 GL) (GE Healthcare Biosciences, Piscataway, NJ, USA) attached to an AKTApure 25 system (GE Healthcare Biosciences). The protein was eluted using a linear NaCl gradient of 100–1000 mM NaCl. The protein was then loaded onto a size-exclusion column (HiLoad 16/600 Superdex 200 pg) (GE Healthcare Biosciences) equilibrated in 20 mM Tris-HCl (pH 7.5) and 150 mM NaCl, and fractionated. The purified protein was analyzed by SDS-PAGE and stained with Coomassie Brilliant blue. The protein concentration was determined by using the Bradford assay.

2.3. CD measurements

CD spectra of Rab35 were measured using a JASCO J-1500 CD spectrometer (JASCO Inc., Tokyo, Japan), as described previously [22]. Each solution containing Rab35 was adjusted to a concentration of 5 μM. GTP or GTPγS was added to the Rab35 solution (final concentration, 1, 5, 10 or 50 μM). CD measurements were carried out in a cuvette with a 0.1-cm path length over a temperature range of 10–90 °C. The scanning speed was 100 nm/min with a bandwidth of 1.0 nm and a response time of 0.5 s. The spectra were obtained from 197 to 250 nm and the experiments were repeated three times. Data are shown as mean residue ellipticities. The relative proportions of the secondary structure were estimated from the data using the K2D3 analytical program [23]. Data were analyzed statistically using the Student's *t*-test.

3. Results

3.1. Dynamic structural changes to Rab35 under various environmental conditions

We recorded CD spectra of the recombinant Rab35 protein in buffer containing EDTA under various conditions, including temperature, pH and salt concentration, to investigate physicochemical characteristics of the Rab35 structure without GTP (i.e., stripped) in response to changes from environmental conditions. The proportions of secondary structure content were calculated by using the CD spectra. Under physiological conditions (37 °C, pH 7 and 150 mM NaCl), the CD spectrum of Rab35 showed negative peaks at 208 and 222 nm, which is characteristic for a protein composed of α-helices (Fig. 2A and Table 1).

The CD spectra of Rab35 showed that the α-helix and β-sheet proportions were affected by changes in temperature (Fig. 2A). At lower temperatures, the α-helix content in Rab35 increased and the β-sheet

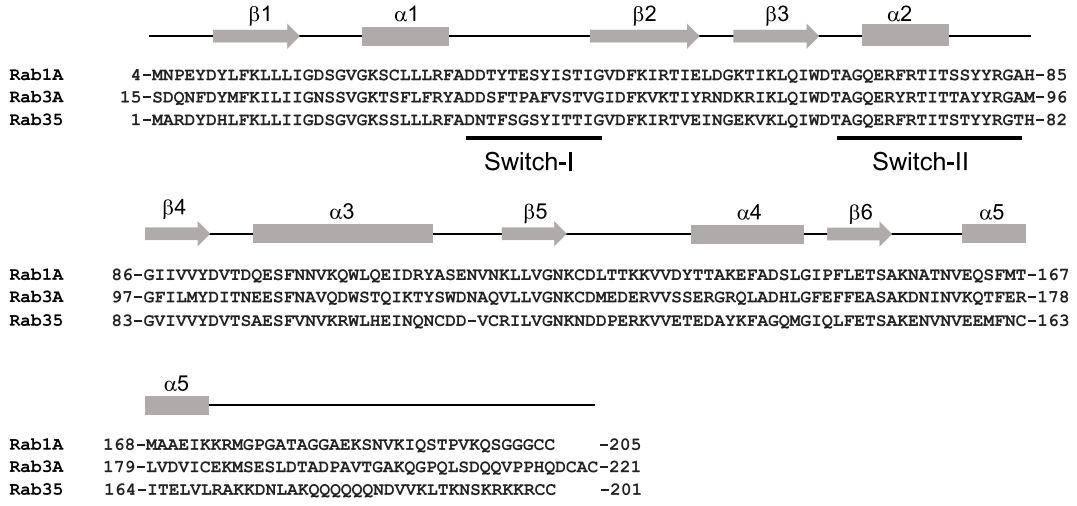

Fig. 1. Sequence alignment of human Rab1a, Rab3a and Rab35. Secondary structure elements corresponding to the Rab3a structure are shown at the top of the sequence with α-helices represented by boxes and β-sheets as arrows. The switch-I and switch-II are shown by lines.

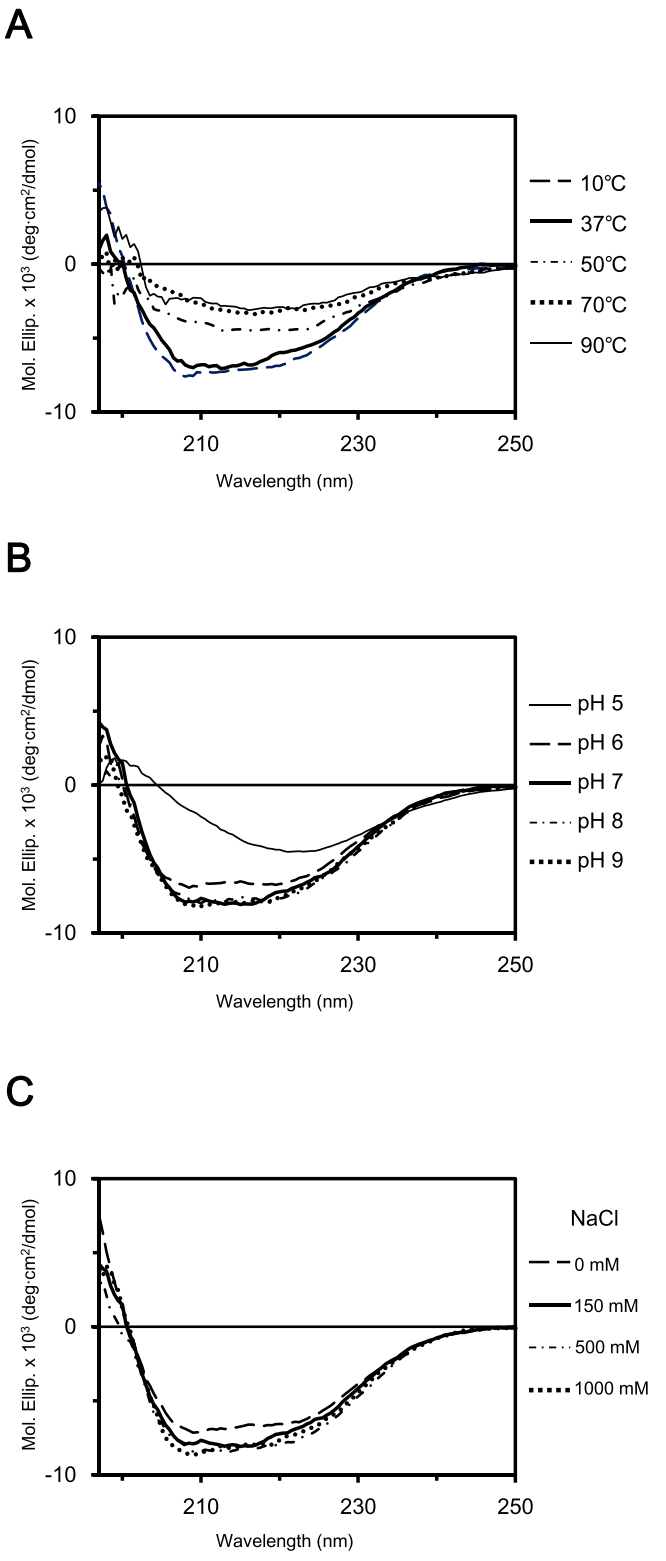

Fig. 2. CD spectra of Rab35 under various environmental conditions. (A) CD spectra of Rab35 in 20 mM sodium phosphate (pH 7), 150 mM NaCl and 5 mM EDTA at different temperatures. The spectra were measured over the temperature range of 10–90 °C. (B) CD spectra of Rab35 in various pH buffers. Buffers were 20 mM acetic acid–sodium acetate (pH 5), 20 mM sodium phosphate (pH 6, 7, 8) or 20 mM boric acid–NaOH buffer (pH 9), containing 150 mM NaCl and 5 mM EDTA. CD spectra were measured at 37 °C. (C) CD spectra of Rab35 at various NaCl concentrations. The buffer used was 20 mM sodium phosphate (pH 7) and 5 mM EDTA containing 0, 150, 500 or 1000 mM NaCl. The spectra were measured at 37 °C.

content decreased. At 10 °C, the α-helix and β-sheet contents were 22.2 ± 2.6% and 29.0 ± 2.8%, respectively (Table 1). However, at higher temperatures, a decrease in the α-helix content of Rab35 was observed, whereas the β-sheet content increased. At 50 °C, the α-helix and the β-sheet contents were 9.2 ± 3.8% and 46.2 ± 3.2%, respectively (Table 1). Above 60 °C, the α-helix content was significantly low (less than 2.5%), whereas the β-sheet content was more than 50%.

We then analyzed structural changes of Rab35 at pH values between 5 and 9. At pH 5, the CD spectrum of Rab35 showed a negative peak at ~217 nm (Fig. 2B), indicating that the predominant secondary structure was β-sheet. The α-helix content was determined to be 3.2 ± 1.3%, which is much lower than observed at other pH values (Table 1). At pH 6, 7, 8 and 9, negative peaks at 208 and 222 nm were observed in the CD spectra, and there was no significant change in the α-helix and β-sheet contents (Fig. 2B and Table 1). These results suggested that the secondary structure of Rab35 was maintained under these pH conditions.

We next analyzed the CD spectra of Rab35 at 37 °C in the presence of different NaCl concentrations (0, 150, 500 and 1000 mM). The CD spectra of Rab35 indicated the presence of α-helix and β-sheet secondary structures at the various salt concentrations examined, including under physiological salt conditions, that is, 150 mM (Fig. 2C). The α-helix and β-sheet contents at each salt concentration were similar (Table 1). Thus, changing the salt concentration had minimal effect on the structure of Rab35, indicating that there were no intra-molecular electrostatic interactions.

3.2. *Effect of GTP on the secondary structure of Rab35*

To study the effect of GTP on the Rab35 secondary structure, CD spectra of Rab35 were measured in the presence of various concentrations of GTP (Rab35–GTP) under physiological conditions, and the CD data were used to estimate the α-helix and β-sheet contents (Fig. 3A and Table 2). Addition of 1 μM GTP at a molar ratio of 0.2:1 with Rab35 gave a CD spectrum that was similar to the CD spectrum recorded for Rab35 in the absence of GTP. However, the addition of >5 μM GTP caused a change in the CD spectrum with an increase in the α-helix content when compared with CD spectra of Rab35 in the absence of GTP. After the addition of 10 μM GTP, the content of α-helix was 19.8 ± 1.3%. Increasing the molar ratio of added GTP to Rab35 from 1:1 to 10:1 did not significantly change the α-helix content. We also analyzed the CD spectra and the secondary structure content of Rab35 when GTPγS, a non-hydrolyzed G-protein GTP analog (Rab35–GTPγS), was added to the solution (Table 2). The α-helix content of Rab35 increased in the presence of 1 μM GTPγS. The α-helix content of Rab35 increased further in the presence of 5 μM GTPγS. The addition GTPγS above 5 μM did not change the α-helix content of Rab35, which is a similar observation made when GTP was added at concentrations above 5 μM. These results suggested that GTP binding stabilized the α-helix structure of Rab35.

We then analyzed the secondary structure of Rab35–GTP under various environmental conditions. Firstly, we measured the CD spectrum of Rab35–GTP at various temperatures (Fig. 3B). The α-helix content of Rab35–GTP increased significantly from that of Rab35 alone at ~37 °C; however, a significant increase in the α-helix content of Rab35–GTP was not observed at high temperatures; >50 °C (Tables 1 and 3).

Next, the CD spectra of Rab35–GTP at different pH values (pH 5 to 9) were measured (Fig. 3C). At pH 5, the α-helix content of Rab35–GTP was markedly low and no secondary structural changes following addition of GTP were observed at this pH (Fig. 4A, Table 3). At pH 7, the α-helix content of Rab35–GTP increased in comparison with that of Rab35 alone, which was also observed at pH 6 (Fig. 4A, Tables 1 and 3). However, GTP addition had no effect on the α-helix content of Rab35 at either pH 8 or 9. Lastly, we also measured CD spectra of Rab35–GTP at various NaCl concentrations: 0, 150, 500 and 1000 mM (Fig. 3D). An increase in the α-helix content of Rab35 after the addition of GTP was observed in the presence of 150 mM NaCl; however, we could not detect

Table 1
Secondary structure composition (as %) of Rab35 at different temperatures, pH values and salt concentrations.

GTP (−)										
	Temperature (°C)									
	10	**20**	**30**	**37**	**40**	**50**	**60**	**70**	**80**	**90**
α-Helix	22.2 (2.6)	21.4 (4.1)	18.5 (1.1)	14.2 (2.1)	5.5 (1.6)	9.2 (3.8)	2.7 (1.9)	2.2 (1.4)	5.0 (2.5)	2.5 (1.9)
β-Sheet	29.0 (2.8)	31.4 (2.6)	35.0 (5.5)	40.2 (3.8)	47.2 (2.4)	46.2 (3.2)	55.1 (3.9)	57.5 (2.1)	51.4 (2.0)	54.1 (4.4)
Random	48.8 (2.1)	47.2 (1.7)	44.5 (2.2)	45.6 (1.9)	47.3 (2.5)	44.6 (0.9)	42.2 (2.0)	40.3 (1.0)	43.7 (1.2)	43.4 (3.3)

	pH				
	5	**6**	**7**	**8**	**9**
α-Helix	3.2 (1.3)	12.3 (3.0)	14.2 (2.1)	14.2 (3.9)	17.3 (4.5)
β-Sheet	45.6 (2.6)	38.3 (4.3)	40.2 (3.8)	37.2 (0.4)	37.8 (3.8)
Random	51.2 (1.2)	49.4 (1.5)	45.6 (1.9)	48.7 (3.9)	44.9 (3.1)

	NaCl (mM)			
	0	**150**	**500**	**1000**
α-Helix	19.7 (0.6)	14.2 (2.1)	17.9 (1.9)	14.5 (2.9)
β-Sheet	38.6 (0.6)	40.2 (3.8)	33.0 (6.3)	41.5 (3.4)
Random	41.7 (0.4)	45.6 (1.9)	49.1 (5.0)	44.0 (2.0)

Values are the mean (SD) of three experiments.

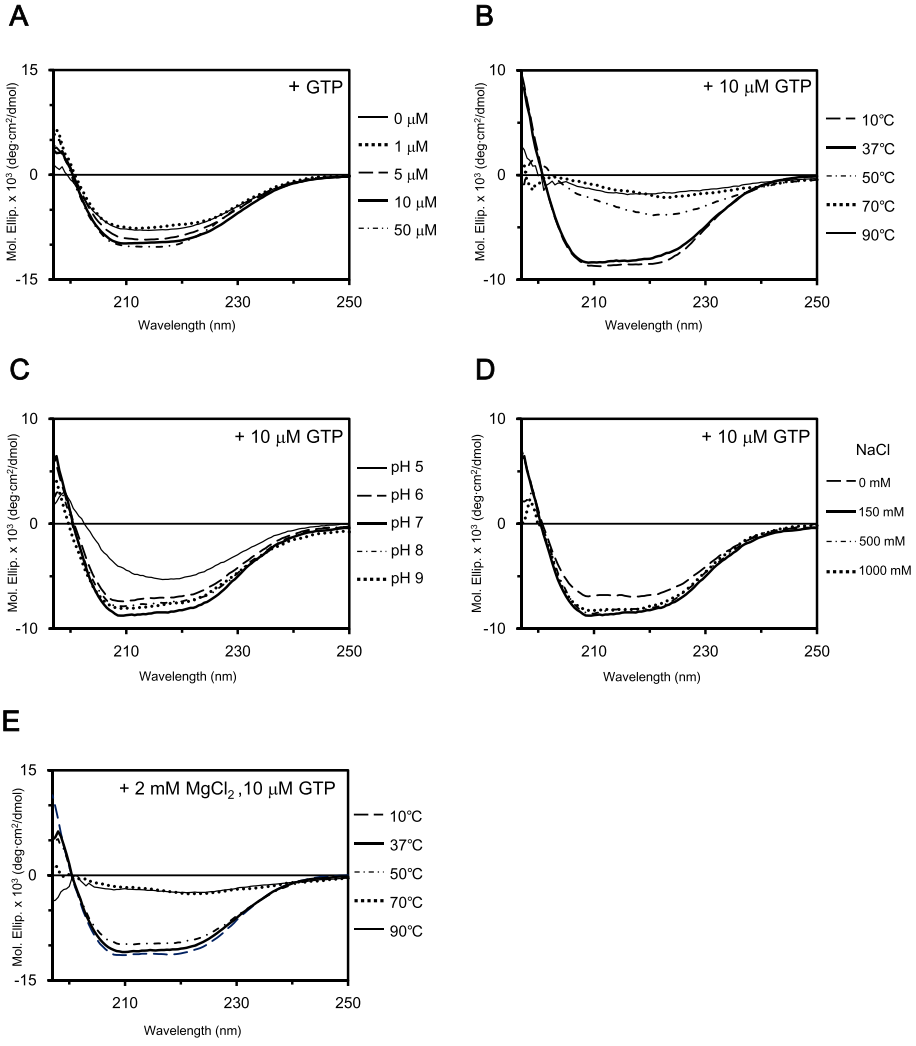

Fig. 3. The effect of GTP on the secondary structure of Rab35 under different environmental conditions. (A) CD spectra of Rab35 with added GTP in a buffer (20 mM sodium phosphate (pH 7), 150 mM NaCl) at 37 °C. The final concentrations of added GTP were 1, 5, 10 and 50 μM. (B) CD spectra of Rab35 with 10 μM GTP added in 20 mM sodium phosphate (pH 7), and 150 mM NaCl at different temperatures. The spectra were measured over the temperature range of 10–90 °C. (C) CD spectra of Rab35 with 10 μM GTP added in various pH buffers (from pH 5 to 9) containing 150 mM NaCl. The spectra were measured at 37 °C. (D) CD spectra of Rab35 with 10 μM GTP added in various NaCl-containing buffers (0, 150, 500 or 1000 mM NaCl) at pH 7. The spectra were measured at 37 °C. (E) CD spectra of Rab35 with 10 μM GTP added in 20 mM sodium phosphate (pH 7), 150 mM NaCl and 2 mM $MgCl_2$ at different temperatures. The spectra were measured over the temperature range of 10–90 °C.

an increase in α-helix content at 0, 500 and 1000 mM NaCl (Fig. 4B, Tables 1 and 3).

Furthermore, we measured CD spectra of Rab35–GTP in buffer containing Mg^{2+}, which enhances the affinity of Rab GTPases toward GTP, at various temperatures (Fig. 3E). Below 37 °C, the CD spectra of Rab35–GTP in the presence of Mg^{2+} were similar to those of Rab35–GTP in the absence of Mg^{2+}, whereas the spectrum of Rab35–GTP in the presence of Mg^{2+} at 50 °C differed to the spectrum recorded on

Table 2
Secondary structure composition (as %) of Rab35 in the presence of GTP or GTPγS at 37 °C.

Reagents		Concentration (μM)				
		0	1	5	10	50
GTP	α-Helix	12.6	16.9	20.5	19.8	20.5
		(0.9)	(7.6)	(3.3)	(1.3)	(6.4)
	β-Sheet	41.5	26.7	38.0	39.2	37.3
		(2.3)	(4.0)	(2.9)	(2.1)	(7.7)
	Random	46.8	56.3	41.5	41.0	42.2
		(2.9)	(3.8)	(0.4)	(1.1)	(4.8)
GTPγS	α-Helix		20.2	25.5	27.0	24.4
			(1.9)	(0.8)	(2.3)	(4.1)
	β-Sheet		36.6	29.3	29.5	33.4
			(2.7)	(0.4)	(2.1)	(3.5)
	Random		43.2	45.2	43.5	42.2
			(0.8)	(0.4)	(0.7)	(0.6)

Values are the mean (SD) of three experiments.

Rab35–GTP without Mg^{2+}. Here, the α-helix content of Rab35–GTP in the presence of Mg^{2+} at 50 °C increased significantly (Tables 1 and 4).

4. Discussion

The GTPase Rab35 is an important factor in intracellular membrane trafficking and many other cellular processes. Rab35 dysfunction is considered to be linked to various diseases such as cancer and neurodegenerative diseases. Thus, Rab35 has attracted attention as a potential biomarker for disease prediction. Rab35 exhibits a Ras-like structure and contains a globular G-domain, which recognizes GTP, GDP and other effector proteins.

The Rab35 structure consists of six β-sheets that form a core surrounded by five α-helices [24]. Our CD experiments under various temperature conditions showed that the α-helices may be less thermally stable than the β-sheets in Rab35 (Table 1). These results of the temperature-dependent changes in Rab35 secondary structure are characteristic, because for most proteins, both the α-helix and β-sheet contents decrease with increasing temperature due to denaturation [25].

The addition of GTP increased the α-helix content of Rab35 at the physiological temperature. The binding of GTP stabilizes the switch-I and switch-II regions to maintain Rab GTPase in the active state (Fig. 1). These two regions are located on the surface of Rab35. Therefore, GTP binding may enhance the structural stability of the α-helices in Rab35, thus providing thermal stability. The addition of GTPγS increased the α-helix content of Rab35 at lower concentrations than GTP. The addition of GTPγS is more effective because GTPγS is not hydrolyzed, whereas a fraction of GTP may be hydrolyzed during the measurement with GTP present. The thermal stability of Rab35–GTP was promoted by Mg^{2+}, because the presence of this cation enhances the affinity of Rab35 toward GTP.

Next, we investigated the pH effects on the structure of Rab35 bound with GTP. Changing the pH revealed that the α-helices of Rab35 were most stable between pH 6 and 7. No stabilization of α-helices by GTP was observed under basic conditions (pH 8 and 9). Then, when the salt concentration of the buffer was changed, stabilization of the α-helices was observed at the physiological salt concentration following the addition of GTP, but this effect was absent at non-physiological salt concentrations. This indicates that the stabilization of the Rab35 structure by GTP is more effective in an environment that closely matches physiological conditions.

The crystal structures of Rab35-effector protein complexes (Rab35–ACAP2 and Rab35–RUSC2) and the Rab35-GEF complex (Rab35–DENND1B) have been solved, but the structure of Rab35 alone has not been solved [20,24]. GTP was bound to Rab35 in the Rab35-effector protein complexes, whereas GTP was not bound to Rab35 in the Rab35-GEF complex. In the all complexes, Rab35 adopts a conserved G-domain structure composed of five α-helices and six β-sheets, which is observed for other GTPases. Based on the crystal structures of Rab35, there is almost no change in the secondary structure of Rab35 upon binding GTP. Conversely, dynamic structural changes to Rab35 upon interaction with GTP were detected in solution by the CD spectroscopic results presented herein.

The function of Rab35 in recycling endosome trafficking toward the plasma membrane is achieved by recruitment effector proteins to the endosomal membrane and is dependent on GTP binding. Lin et al. presented the structures of Rab35 in complex with effector proteins centaurin-β2 and RUSC2 [20]. These effector proteins recognize Rab35 through the switch-I and switch-II regions (Fig. 1), and the interswitch region of switch-I and switch-II. Centaurin-β2 is an Arf GTPase activating protein, and D721 of centaurin-β2 forms a hydrogen bond with T72 of Rab35, which is located in the α-helix of the switch-II region [20]. A recent study revealed that T72 is phosphorylated by the leucine-rich repeat kinase 2 (LRRK2), which is a factor in the pathogenesis of Parkinson's disease [26–28]. Mutation of T72 to either alanine or aspartic acid impaired the interactions between Rab35 and centaurin-β2, inducing the degeneration of dopaminergic neurons [20,29]. The stability of the α-helix may facilitate the interaction between Rab35 and centaurin-β2 via T72. Therefore, changes in the conformation of Rab35 caused by external environmental conditions may influence the interaction of Rab35 with effector biomolecules.

Table 3
Secondary structure components (as %) of Rab35 with GTP at various temperatures, pH values or salt concentrations.

10 μM GTP										
	Temperature (°C)									
	10	**20**	**30**	**37**	**40**	**50**	**60**	**70**	**80**	**90**
α-Helix	24.1 (0.6)	22.3 (0.7)	20.0 (1.7)	19.8 (1.3)	17.5 (1.7)	6.2 (1.5)	1.5 (0.7)	2.0 (1.2)	1.8 (1.3)	1.6 (1.0)
β-Sheet	34.5 (0.8)	36.0 (0.7)	38.6 (0.9)	39.2 (2.1)	40.5 (1.1)	49.2 (1.6)	57.3 (0.7)	55.8 (0.5)	57.0 (2.4)	56.7 (1.4)
Random	41.4 (0.7)	41.7 (1.0)	41.4 (1.1)	41.0 (1.1)	42.0 (0.9)	44.6 (1.4)	41.2 (0.6)	42.2 (1.0)	41.2 (1.8)	41.7 (1.3)
	pH									
	5	**6**	**7**	**8**	**9**					
α-Helix	2.7 (0.1)	20.9 (0.5)	19.8 (1.3)	18.5 (4.1)	19.1 (1.9)					
β-Sheet	41.5 (0.4)	29.7 (3.9)	39.2 (2.1)	35.5 (4.2)	38.8 (3.2)					
Random	55.8 (0.5)	49.3 (3.4)	41.0 (1.1)	46.1 (0.6)	42.1 (1.9)					
	NaCl (mM)									
	0	**150**	**500**	**1000**						
α-Helix	15.5 (0.9)	19.8 (1.3)	14.2 (1.7)	12.9 (2.0)						
β-Sheet	43.0 (0.3)	39.2 (2.1)	39.3 (1.0)	41.3 (3.1)						
Random	41.5 (1.1)	41.0 (1.1)	46.5 (1.4)	45.8 (2.2)						

Values are the mean (SD) of three experiments.

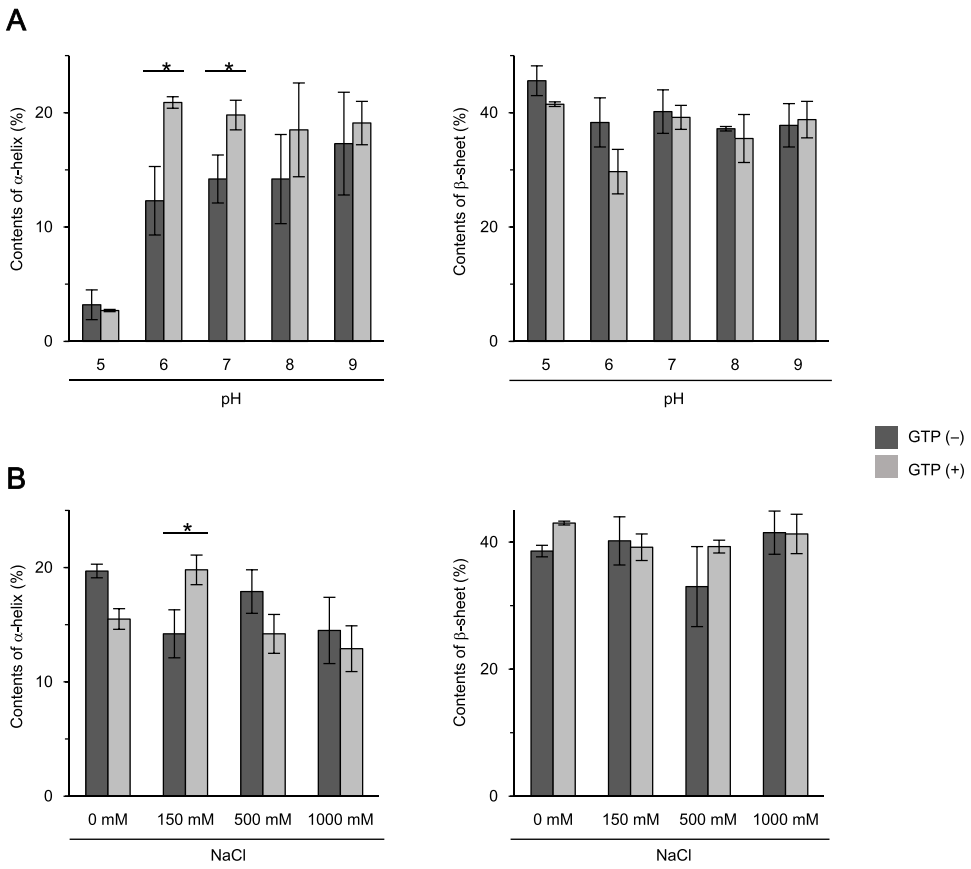

Fig. 4. Secondary structure of Rab35 under various environmental conditions. (A) α-Helix and β-sheet contents for Rab35 estimated from the CD spectra of Rab35 and Rab35–GTP at various pH values. (B) α-Helix and β-sheet contents for Rab35 estimated from the CD spectra of Rab35 and Rab35–GTP under different salt concentrations. Data are mean ± S.D. ($n = 3$), $^*P < 0.05$.

Table 4
Secondary structure components (as %) of Rab35 in the presence of GTP and Mg^{2+} at various temperatures.

10 μM GTP, Mg^{2+}										
	Temperature (°C)									
	10	**20**	**30**	**37**	**40**	**50**	**60**	**70**	**80**	**90**
α-Helix	27.3 (1.1)	26.9 (1.9)	27.5 (1.4)	22.5 (2.7)	21.0 (3.3)	17.1 (2.1)	6.5 (3.4)	1.9 (1.1)	2.6 (2.3)	0.8 (1.1)
β-Sheet	25.8 (1.4)	28.1 (2.0)	27.3 (1.6)	34.5 (4.0)	32.4 (5.2)	39.0 (1.9)	51.9 (6.3)	56.9 (2.2)	57.0 (5.2)	59.7 (3.8)
Random	46.9 (0.9)	45.0 (2.0)	45.6 (1.7)	43.0 (0.8)	46.6 (2.6)	43.9 (1.4)	41.6 (3.4)	41.2 (1.2)	40.4 (3.0)	39.5 (3.4)

Values are the mean (SD) of three experiments.

The results of this study demonstrated the physicochemical characteristics of the dynamic structure of Rab35. In this research, we showed that changes in the external environmental conditions caused structural changes to Rab35, especially to the α-helices region. Furthermore, we found that GTP stabilizes the secondary structure of Rab35 when temperature, pH and salt concentration are within a physiological range. We showed that changes of structures and physicochemical characteristics influence the interaction of Rab35 with effector biomolecules, and therefore regulate the function of Rab35 in membrane trafficking.

Funding

This work was supported by research activity of Teikyo University.

CRediT authorship contribution statement

Takuya Murata: Investigation, Formal analysis, Writing - original draft. **Yuka Unno:** Writing - review & editing. **Mitsunori Fukuda:** Resources, Writing - review & editing. **Naoko Utsunomiya-Tate:** Writing - review & editing, Project administration.

Appendix A. Supplementary data

Supplementary data to this article can be found online at https://doi.org/10.1016/j.bbrep.2020.100776.

References

[1] H. Stenmark, V.M. Olkkonen, The Rab GTPase family, Genome Biol. 2 (2001) 1–7, reviews3007.
[2] H. Stenmark, Rab GTPases as coordinators of vesicle traffic, Nat. Rev. Mol. Cell Biol. 10 (2009) 513–525.
[3] M. Zerial, H. McBride, Rab proteins as membrane organizers, Nat. Rev. Mol. Cell Biol. 2 (2001) 107–118.
[4] Y. Zhen, H. Stenmark, Cellular functions of Rab GTPases at a glance, J. Cell Sci. 128 (2015) 3171–3176.
[5] M. Fukuda, Regulation of secretory vesicle traffic by Rab small GTPases, Cell, Mol. Life Sci. 65 (2008) 2801–2813.
[6] M. Chaineau, M.S. Ioannou, P.S. McPherson, Rab35: GEFs, GAPs and effectors, Traffic 14 (2013) 1109–1117.
[7] E.P. Lamber, A.C. Siedenburg, F.A. Barr, Rab regulation by GEFs and GAPs during membrane traffic, Curr. Opin. Cell Biol. 59 (2019) 34–39.
[8] O. Pylypenko, H. Hammich, I.M. Yu, A. Houdusse, Rab GTPases and their interacting protein partners: structural insights into Rab functional diversity, Small GTPases 9 (2018) 22–48.

[9] B.L. Grosshans, D. Ortiz, P. Novick, Rabs and their effectors: achieving specificity in membrane traffic, Proc. Natl. Acad. Sci. U. S. A 103 (2006) 11821–11827.
[10] A.K. Gillingham, R. Sinka, I.L. Torres, K.S. Lilley, S. Munro, Toward a comprehensive map of the effectors of Rab GTPases, Dev. Cell 31 (2014) 358–373.
[11] F.R. Kiral, F.E. Kohrs, E.J. Jin, P.R. Hiesinger, Rab GTPases and membrane trafficking in neurodegeneration, Curr. Biol. 28 (2018) R471–R486.
[12] X.Z. Yang, X.X. Li, Y.J. Zhang, L. Rodriguez-Rodriguez, M.Q. Xiang, H.Y. Wang, X. F.S. Zheng, Rab1 in cell signaling, cancer and other diseases, Oncogene 35 (2016) 5699–5704.
[13] I. Kouranti, M. Sachse, N. Arouche, B. Goud, A. Echard, Rab35 regulates an endocytic recycling pathway essential for the terminal steps of cytokinesis, Curr. Biol. 16 (2006) 1719–1725.
[14] K. Klinkert, M. Rocancourt, A. Houdusse, A. Echard, Rab35 GTPase couples cell division with initiation of epithelial apico-basal polarity and lumen opening, Nat. Commun. 7 (2016) 11166.
[15] J. Chevallier, C. Koop, A. Srivastava, R.J. Petrie, N. Lamarche-Vane, J.F. Presley, Rab35 regulates neurite outgrowth and cell shape, FEBS Lett. 583 (2009) 1096–1101.
[16] H. Kobayashi, M. Fukuda, Rab35 regulates arf6 activity through centaurin-β2 (ACAP2) during neurite outgrowth, J. Cell Sci. 125 (2012) 2235–2243.
[17] H. Kobayashi, M. Fukuda, Rab35 establishes the EHD1-association site by coordinating two distinct effectors during neurite outgrowth, J. Cell Sci. 126 (2013) 2424–2435.
[18] M. Fukuda, H. Kobayashi, K. Ishibashi, N. Ohbayashi, Genome-wide investigation of the Rab binding activity of RUN domains: development of a novel tool that specifically traps GTP-Rab35, Cell Struct. Funct. 36 (2011) 155–170.
[19] D. Dambournet, M. Machicoane, L. Chesneau, M. Sachse, M. Rocancourt, A. El Marjou, E. Formstecher, R. Salomon, B. Goud, A. Echard, Rab35 GTPase and OCRL phosphatase remodel lipids and F-actin for successful cytokinesis, Nat. Cell Biol. 13 (2011) 981–988.
[20] L. Lin, Y. Shi, M. Wang, C. Wang, J. Zhu, R. Zhang, Rab35/ACAP2 and Rab35/RUSC2 complex structures reveal molecular basis for effector recognition by Rab35 GTPase, Structure 27 (2019) 1–12.
[21] J.J. Dumas, Z. Zhu, J.L. Connolly, D.G. Lambright, Structural basis of activation and GTP hydrolysis in Rab proteins, Structure 7 (1999) 413–423.
[22] N. Tochio, T. Murata, N. Utsunomiya-Tate, Effect of site-specific amino acid D-isomerization on β-sheet transition and fibril formation profiles of Tau microtubule-binding repeat peptides, Biochem. Biophys. Res. Commun. 508 (2019) 184–190.
[23] C. Louis-Jeune, M. Andrade-Navarro, C. Perez-Iratxeta, Prediction of protein secondary structure from circular dichroism using theoretically derived spectra, Proteins: Struct. Funct. Bioinf. 80 (2012) 374–381.
[24] X. Wu, M.J. Bradley, Y. Cai, D. Kummel, E.M. De La Cruz, F.A. Barr, K.M. Reinisch, Insights regarding guanine nucleotide exchange from the structure of a DENN-domain protein complexed with its Rab GTPase substrate, Proc. Natl. Acad. Sci. U. S. A 108 (2011) 18672–18677.
[25] K. Sakai-Kato, A. Ishiguro, K. Mikoshiba, J. Aruga, N. Utsunomiya-Tate, CD spectra show the relational style between Zic-, Gli-, Glis-zinc finger protein and DNA, Biochim. Biophys. Acta 1784 (2008) 1011–1019.
[26] M. Steger, F. Diez, H.S. Dhekne, P. Lis, R.S. Nirujogi, O. Karayel, F. Tonelli, T. N. Martinez, E. Lorentzen, S.R. Pfeffer, D.R. Alessi, M. Mann, Systematic proteomic analysis of LRRK2-mediated Rab GTPase phosphorylation establishes a connection to ciliogenesis, eLife 6 (2017), e31012.
[27] W. Seol, D. Nam, I. Son, Rab GTPases as physiological substrates of LRRK2 kinase, Exp. Neurobiol. 28 (2019) 134–145.
[28] E.J. Bae, D.K. Kim, C. Kim, M. Mante, A. Adame, E. Rockenstein, A. Ulusoy, M. Klinkenberg, G.R. Jeong, J.R. Bae, C. Lee, H.J. Lee, B.D. Lee, D.A. Di Monte, E. Masliah, S.J. Lee, LRRK2 kinase regulates α-synuclein propagation via RAB35 phosphorylation, Nat. Commun. 9 (2018) 1–15.
[29] G.R. Jeong, E.H. Jang, J.R. Bae, S. Jun, H.C. Kang, C.H. Park, J.H. Shin, Y. Yamamoto, K. Tanaka-Yamamoto, V.L. Dawson, T.M. Dawson, E.M. Hur, B. D. Lee, Dysregulated phosphorylation of Rab GTPases by LRRK2 induces neurodegeneration, Mol. Neurodegener. 13 (2018) 8.